OPEN

Txnip Gene Knockout Ameliorated High-Fat Diet–Induced Cardiomyopathy Via Regulating Mitochondria Dynamics and Fatty Acid Oxidation

Aiyun Li, DSc, Yichao Zhang, BS,* Jin Wang, DSc,* Yan Zhang, MSc,* Wanzhen Su, BM,* Feng Gao, MM,† and Xiangying Jiao, PhD**

Abstract: Epidemic of obesity accelerates the increase in the number of patients with obesity cardiomyopathy. Thioredoxin interacting protein (TXNIP) has been implicated in the pathogenesis of multiple cardiovascular diseases. However, its specific role in obesity cardiomyopathy is still not well understood. Here, we evaluated the role of TXNIP in obesity-induced cardiomyopathy by feeding wild-type and *txnip* gene knockout mice with either normal diet or high-fat diet (HFD) for 24 weeks. Our results suggested that TXNIP deficiency improved mitochondrial dysfunction via reversing the shift from mitochondrial fusion to fission in the context of chronic HFD feeding, thus promoting cardiac fatty acid oxidation to alleviate chronic HFD-induced lipid accumulation in the heart, and thereby ameliorating the cardiac function in obese mice. Our work provides a theoretical basis for TXNIP exerting as a potential therapeutic target for the interventions of obesity cardiomyopathy.

Key Words: TXNIP, obesity cardiomyopathy, mitochondria dynamic, fatty acids oxidation

(*J Cardiovasc Pharmacol*™ 2023;81:423–433)

Received for publication January 11, 2023; accepted February 23, 2023.

From the *Key Laboratory of Cellular Physiology (Shanxi Medical University), Ministry of Education, and the Department of Physiology, Shanxi Medical University, Taiyuan, China; and †Sixth Clinical Medical College of Shanxi Medical University, Taiyuan, China.

Supported by the Youth Project of Applied Basic Research Program in Shanxi Province (No. 202103021223212) and Science Research Start-up Foundation for Doctor of Shan xi Medical University (No. XD2012).

The authors report no conflicts of interest.

Supplemental digital content is available for this article. Direct URL citations appear in the printed text and are provided in the HTML and PDF versions of this article on the journal's Web site (www.jcvp.org).

A. Li and Y. Zhang have contributed equally and should be considered co-first authors.

Conceptualization: A. Li, Y. Zhang, F. Gao, and X. Jiao. Data curation: Y. Zhang and W. Su. Investigation: Y. Zhang and W. Su. Methodology: A. Li and Y. Zhang. Project administration: J. Wang. Resources: J. Wang. Software: Y. Zhang. Supervision: X. Jiao and F. Gao. Writing—original draft: Y. Zhang. Writing—review and editing: A. Li and X. Jiao.

Reprints: Feng Gao, MM, Sixth Clinical Medical College of Shanxi Medical University 7 Yingxin Rd, Taiyuan, 030003 China (e-mail: tgzyygf@163.com) or Xiangying Jiao, PhD, Department of Physiology, Shanxi Medical University, 56 Xinjian South Rd, Taiyuan 030001, China (e-mail: jiaoxyty@163.com).

INTRODUCTION

The World Health Organization defines overweight and obesity as a pathological condition in which excess or abnormal fat accumulates in body, although reduced physical activity, unhealthy eating habits, stress, and fear can exacerbate obesity, especially during the COVID-19 pandemic.[1,2] Obesity is considered to affect myocardial structure and pump performance and result in a unique disease entity termed obesity cardiomyopathy. Obesity cardiomyopathy is defined as myocardial disease that cannot be explained by diabetes, hypertension, coronary artery disease, or other causes in obese individuals.[3] Researches showed that chronic metabolic disorders because of obesity contribute to oxidative stress, inflammation, insulin resistance, lipid toxicity, and energy deficiency, all of which may result in the progression of heart failure.[4] However, the specific link between cardiac metabolism and obesity cardiomyopathy remains elusive. Besides, the current treatment for obesity cardiomyopathy is focused on management of obesity[5] and there are still no specific targets available for the treatment of obesity cardiomyopathy.

Heart is described as "metabolic omnivore" because of its metabolic flexibility that can obtain energy from various circulating substrates.[6] Under normal conditions, heart relies mainly (~80%) on fatty acid oxidation (FAO) to promote adenosine triphosphate (ATP) production, followed by glucose oxidation (~12%) and with other substrates supply the rest.[4] However, a large amount of lipids will accumulate in the heart (also termed as cardiac lipotoxicity) when the substrate supply exceeds the demand for ATP synthesis, leading to cardiac dysfunction.[7] Given that increased cardiac FAO could induce cardiac dysfunction in obese models through oxidative damage and mitochondrial dysfunction,[8] recent study reported that increasing cardiac FAO could preserve cardiac function in diet-induced obese mice.[9] Besides, previous studies have shown that chronic increases in myocardial glucose uptake and oxidation to prevent high FAO caused cardiac dysfunction in diet-induced obesity.[10] These evidences illuminated that increased FAO per se may not be the factor that contribute to cardiac lipotoxicity, whereas impaired metabolic flexibility in the heart and the imbalance between cardiac fatty acid uptake and oxidation may be the cause of heart dysfunction.[11]

Mitochondria are especially abundant in the heart tissue because of its constant high-energy demands, and mitochondrial dysregulation is thought to play a rather unique role in

cardiovascular diseases.[12] Mitochondrial dysfunction can result in a lack of intracellular ATP in obesity because of disturbances in cellular energy metabolism and lead to accumulation of reactive oxygen species (ROS) that drive oxidative stress.[13,14] Indeed, excess lipid accumulation and fatty acid oxidation has been found to induce ROS production in the mitochondrial respiratory chain and contribute to mitochondrial dysfunction.[15] Besides, mitochondrial dynamics is closely related to mitochondrial function, and a fine balance between fusion and fission is critical in the progression of cardiovascular diseases.[16,17] It is showed that impaired mitochondrial dynamics contributed to mitochondrial dysfunction and thus resulted in heart dysfunction induced by a high-fat diet (HFD).[18] Previous study showed that lipid overload in the heart induced mitochondrial ROS generation and thus caused mitochondrial dysfunction via regulating of mitochondrial dynamics.[19] Thus, finding ways to protect mitochondrial function from excessive oxidative damage and disrupted mitochondrial dynamics, and meanwhile increase FAO in the heart, will be an interesting perspective for the intervention of obesity cardiomyopathy.

Thioredoxin-interacting protein (TXNIP) is a multifunctional protein linking pathways of antioxidant defense and energy metabolism. TXNIP is an endogenous inhibitor of the thioredoxin (Trx) antioxidant system by binding to Trx and blocks its antioxidant function.[20] Besides, TXNIP also serves as a switch of energy metabolism to regulate the process of glucose and lipid metabolism.[21–24] TXNIP has been implicated in cardiovascular pathology, such as myocardial ischemia, ischemia-reperfusion injury, pressure overload, and cardiac hypertrophy.[25–29] Previous research has found that cardiomyocyte-specific *txnip* gene knockout (KO) enhanced cardiac FAO.[30] However, the underlying correlation between TXNIP and obesity cardiomyopathy had not yet been reported. In the present study, a long-term HFD-induced obesity model was established and the results demonstrated that deletion of TXNIP is sufficient to prevent obesity cardiomyopathy via regulating mitochondria dynamics and facilitating FAO. These findings indicate that TXNIP plays a crucial role in obesity cardiomyopathy and may serve as a potential drug target for its clinical therapy.

MATERIALS AND METHODS

Animals

Txnip systemic deficiency heterozygous mice (MGI: 1889549; GemPharmatech Co, Ltd, Jiangsu, China) in the C57BL/6J background were originally generated using sgRNA&CRISPR/Cas9 technology (Table 1). *Txnip*-deficient homozygous (also named KO) mice and wild-type (WT) littermate mice were verified by polymerase chain reaction (PCR; see **Figure S1**, **Supplemental Digital Content**, http://links.lww.com/JCVP/A925), and the primer sequences for PCR are showed in **Supplemental Digital Content** (see **Table S1**, http://links.lww.com/JCVP/A928). All mice were bred and kept in a specific pathogen-free facility and reared in standardized settings with unrestricted access to food and water on a fixed 12-hour light and 12-hour darkness cycle. All animal experiments were in accordance with the animal ethics standards of Shanxi Medical University and approved by the ethics committee.

TABLE 1. gRNA Primer Sequences

gRNA Name	gRNA Primer (5′–3′)	PAM
Gps000210-Txnip–S1	ACACGGTGTGCTCCTAGCG	GGG
Gps000210-Txnip–S2	CAACCAATCAGCGAGGCCGC	CGG
Gps000210-Txnip–S3	GGTCTCCGGCTTCAAG	TGG
Gps000210-Txnip–S4	CTATGCCACAGTGCGGGCAC	TGG

At the age of 4 weeks, male KO mice and WT littermate mice were randomly divided into four different groups: (1) WT group, (2) KO group, (3) WT-HFD group, and (4) KO-HFD group. Each group was fed either with a normal diet (ND) or with a HFD beginning at the age of 4 weeks and sustained for 24 weeks. Dietary intake for the HFD groups was 5.24 kcal/g, 60 kcal% fat, 20 kcal% carbohydrate, and 20 kcal% protein (D12492; Research Diets Inc). The body weight of mice was recorded weekly. After 24 weeks of treatment, the blood and heart tissue were harvested, and the triglyceride (TG), nonesterified free fatty acids (NEFAs), total cholesterol (TC), low-density lipoprotein cholesterol (LDL-C), and high-density lipoprotein cholesterol (HDL-C) contents in the serum and heart tissue homogenate were determined using commercial quantification kits (Nanjing Jiancheng Bioengineering Institute, Nanjing, China).

Fasting Blood Glucose and Oral Glucose Tolerance Test

Mice were fasted overnight with free access to water. Fasting blood glucose (FBG) was measured from tail vein blood using the OneTouch Ultra glucose meter (Life Scan, Milpitas, CA). For oral glucose tolerance test, all the mice received glucose (2 g/kg body weight) by oral gavage, and blood glucose contents were recorded at 0, 15, 30, 60, 90, and 120 minutes. Besides, the area under curve (AUC) was calculated.

Echocardiography

At the end of feeding, echocardiography was performed using a GE Vivid-7 ultrasound system (General Electric), and serial M-mode echocardiographic pictures of mice were captured. The short-axis views were recorded at the level of the papillary muscles. The left ventricular ejection fraction (LVEF), left ventricular fractional shortening (LVFS), left ventricular internal diameter at end systole (LVIDs), left ventricular internal diameter at end diastole (LVIDd), left ventricular end systolic volume (LVESV), left ventricular end diastolic volume (LVEDV), left ventricular posterior wall thickness at end systole (LVPWs), left ventricular posterior wall thickness at end diastole (LVPWd), interventricular septal thickness at systole (IVSs), and interventricular septal thickness at diastole (IVSd) were used to evaluate cardiac function. The measurements were performed by a single individual who was unaware of the study's design.

Measurement of Superoxide Dismutase Activity and Malondialdehyde and ATP Levels

Heart tissues were homogenated and centrifuged. Superoxide dismutase (SOD) activity and malondialdehyde

TABLE 2. Antibodies Used for Western Blot Analysis

Antibody	Company	Catalog No.	Dilution Ratio
TXNIP	Abcam	ab188865	1:1500
GLUT1	ABclonal	A6982	1:1000
GLUT4	CST	2213s	1:1000
PDHE1α	CST	2784s	1:1000
p-PDHE1α	CST	31866s	1:1000
MFN1	ABclonal	A9880	1:1000
MFN2	ABclonal	A12771	1:1000
OPA1	ABclonal	A9833	1:1000
DRP1	ABclonal	A2586	1:1000
FIS1	ABclonal	A5821	1:1500
Na^+-K^+-ATPase	ABclonal	A7878	1:1500
β-Actin	Bioworld	AP0060	1:10,000

(MDA) and ATP levels in the supernatants were assayed with commercial assay kits according to the manufacturer's protocol and normalized with protein concentrations.

Western Blot Analysis

Heart tissue was homogenized in RIPA buffer mixed with protease inhibitors and protein phosphatase inhibitors to acquire the total protein samples, and the membrane and cytosolic protein were extracted with Membrane Protein Extraction Kit (Solarbio Science & Technology Co, Ltd, Beijing, China). The protein concentration was measured using a BCA Protein Assay Kit (Boster Biological Technology Co, Ltd, Wuhan, China). Proteins were separated by SDS-PAGE gels (Bio-Rad, Shanghai, China) and then transferred to polyvinylidene difluoride membrane (Millipore, Taufkirchen, Germany). The membrane was incubated with specific primary antibodies at 4°C overnight after blocking with 5% bovine serum albumin. The secondary antibody was incubated for 2 hours and the bands on each membrane were then detected using an ultra-sensitive enhanced chemiluminescence detection kit (Seven Biotech, Corp, Ltd, Beijing, China), and the membrane was subsequently exposed using a Bio-Rad ChemiDoc Touch Imaging System. The gray value was examined using the Image J software. The antibodies used in this study are listed in Table 2.

Real-Time Quantitative Polymerase Chain Reaction

Total RNA of heart tissue was extracted using the Trizol kits (TaKaRa Bio Inc, Japan) and reverse-transcribed into cDNA with the QuantiTect Reverse Transcription Kit (TaKaRa Bio Inc). RT-PCR was conducted with a TB Green Premix Ex Taq II (TaKaRa Bio Inc) using a LightCycler 96 System (Roche). β-Actin was used as the internal reference. The $2^{-\Delta\Delta Ct}$ method was used to calculate the fold changes. PCR primer sequences are shown in Table 3.

Electron Microscopy

The heart tissue was fixed in 3% glutaraldehyde, dehydrated with alcohol, and then embedded in epoxy resin. The ultrathin sections were used, and the ultrastructure of mitochondria in different samples was observed by JEM-1400-FLASH transmission electron microscope. Six random fields (×10,000) were captured per heart. The mitochondrial volume density was quantified by dividing the total mitochondrial area by the total tissue area using Image J software.

Mitochondrial Respiratory Complex V Activity

The activity of the mitochondrial respiratory complex V was detected using the commercial kits (Solarbio Science & Technology Co, Ltd) following the manufacturer's instructions. The values were expressed in terms of U/mgprot.

JC-1 Staining Assay

Isolation of mitochondria was performed using Mitochondrial Extraction Kit (Solarbio Science & Technology Co, Ltd). Then, purified mitochondria were added to the 5-fold dilution JC-1 staining working solution as per the instruction of JC-1 Mitochondrial Membrane Potential Detection Kit (Solarbio Science & Technology Co, Ltd). Red and green fluorescence were detected, and the attenuation of the red-to-green fluorescence intensity ratio shows an increase in the depolarization of mitochondrial membrane.

Statistical Analysis

Statistical analysis was performed using the GraphPad Prism 6 software (GraphPad Software, Inc, San Diego, CA). All data are represented as mean ± standard error of the mean. One-way ANOVA followed by the least significant difference post hoc test was used to confirm differences. A value of $P < 0.05$ was considered statistically significant.

TABLE 3. Primer Sequences

Gene	Primer Sequences (5′–3′)
Txnip	F: CAAGGGTCTCAGCAGTGCAAAC
	R: GCTCGAAGCCGAACTTGTACTC
Cd36	F: TGGAGCTGTTATTGGTGCAG
	R: TGGGTTTTGCACATCAAAGA
Cpt1b	F: TGCCCATGTGCTCCTACCAG
	R: GCCCTCATAGAGCCAGACCTTG
Acadm	F: TGATGTGGCGGCCATTAAGA
	R: GGGTTAGAACGTGCCAACAAGAA
Acadl	F: CTACCTCATGCAAGAGCTTCCACA
	R: CTTCAAACATGAACTCACAGGCAGA
Acox1	F: AAGATGGATCCTAAGCCAGCTGAA
	R: CAGCTTACCACAAAGCCAGCTACTC
Hk2	F: GGCTTTCAATCCAGAGCATGAG
	R: CGAGTGCCCAGGGATATGAG
Pfkm	F: ATGCCGCTGTTCGCTCTACC
	R: CTTGACCAGTCCAGCCTCCA
Pkm	F: TCGCAGCAGGAACCGAAGTA
	R: CTTGGTGGCCTCACTTGGAA
β-Actin	F: ACTGGGACGACATGGAGAAG
	R: GGGGTGTTGAAGGTCTCAAA

RESULTS

Txnip Gene KO Ameliorated Cardiac Dysfunction Induced by Long-Term HFD

To evaluate the changes on cardiac function by *txnip* gene KO, echocardiography was performed. As shown in Figure 1, the results showed that LVEF and LVFS were significantly decreased in WT-HFD mice compared with those in WT mice, whereas the decreases in these parameters were significantly restored by *txnip* gene KO (Figs. 1B, C). Besides, LVIDs and LVESV were significantly increased in WT-HFD mice compared with WT mice, and these alterations were slightly reversed by *txnip* gene KO without statistical significance (Figs. 1D, F). However, there was no statistical difference in other cardiac parameters (Figs. 1E, G–K). These results suggested that *txnip* gene KO ameliorated cardiac dysfunction in mice induced by long-term HFD.

In addition, body weight gain was recorded weekly, and the results showed that the 24-week HFD caused excess weight gain, which observed apparent both by body weight and body size. However, the deletion of TXNIP did not show significant effect on body weight gain (see **Figure S2**, **Supplemental Digital Content**, http://links.lww.com/JCVP/A926). Moreover, 24-week HFD increased serum biochemical parameter, such as FBG, TG, NEFAs, TC, HDL-C and LDL-C, and impaired glucose tolerance. However, TXNIP deletion significantly decreased FBG and improved glucose intolerance caused by HFD, although showed no difference in other serum biochemical parameters (see **Figure 2**, **Supplemental Digital Content**, http://links.lww.com/JCVP/A926).

Txnip Gene KO Normalized Cardiac Lipid and ATP Contents in High-Fat Diet Mice

To verify the underlying role of TXNIP in the alteration of cardiac function, we first evaluated TXNIP expression in the

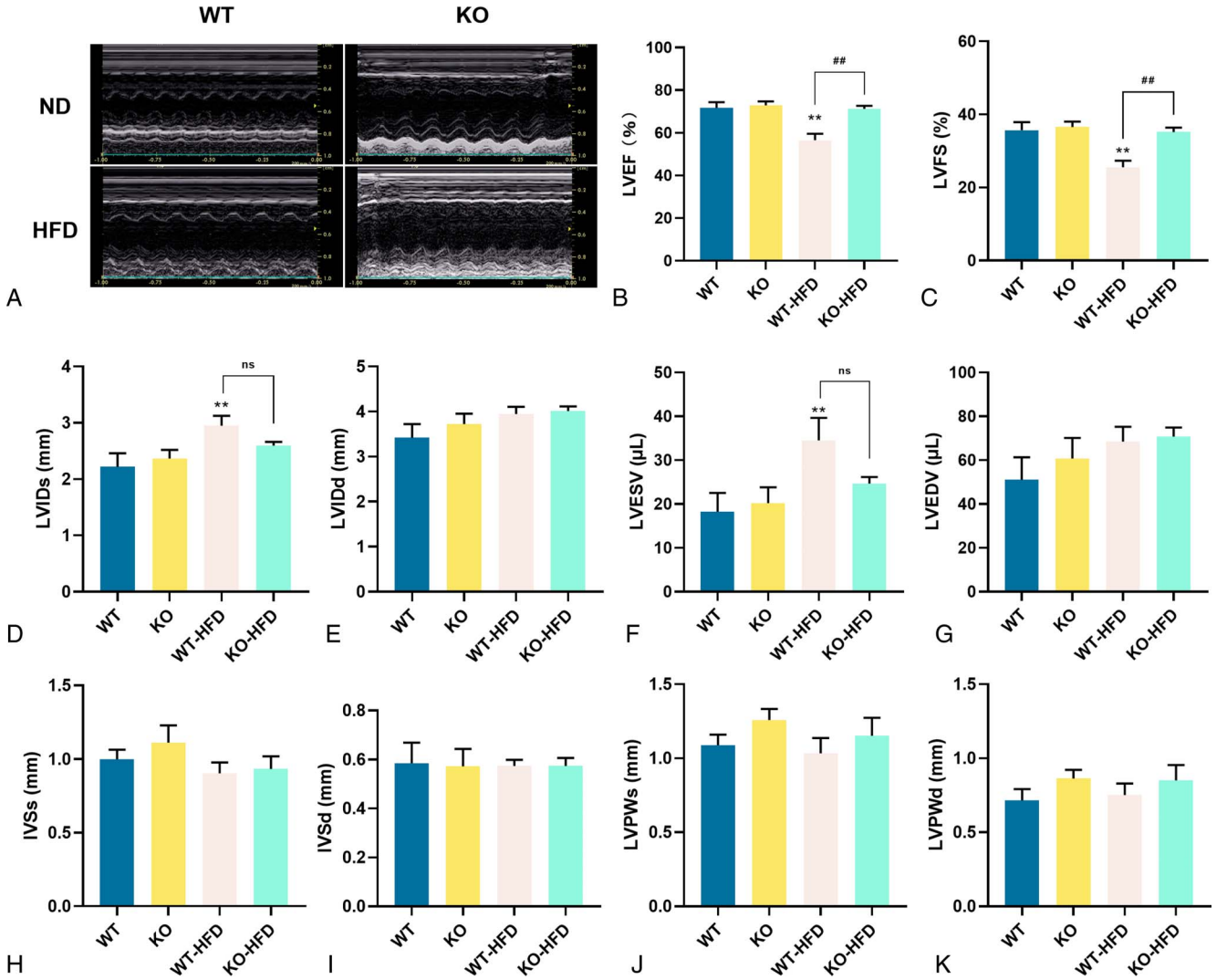

FIGURE 1. *Txnip* gene KO ameliorated the decline in cardiac function induced by a long-term HFD. A, Representative echocardiographic M-mode images of each group at week 24 after treatment. B–K, Parameters of echocardiogram; mean ± SEM, n = 6. $^{**}P < 0.01$ WT-HFD versus WT; $^{\#\#}P < 0.01$ KO-HFD versus WT-HFD. ns, not significant.

heart tissue at both mRNA and protein levels. The results showed that HFD significantly increased TXNIP gene and protein expression in the heart tissue of WT mice, whereas no TXNIP mRNA and slight TXNIP protein bands were detected in the KO mice (Figs. 2A, B), indicating the potential role of TXNIP in cardiac dysfunction induced by long-term HFD. Chronic exposure to dietary lipids is known to promote lipid deposition in the heart, which is the key factor for cardiac dysfunction.[31] Then cardiac lipid contents were evaluated with commercial kits. The results showed that the TG, NEFAs, TC, and LDL-C contents in the heart tissue of WT-HFD mice were significantly increased compared with WT mice, whereas these alterations were obviously reversed by TXNIP deficiency except for TC content. Besides, TXNIP deficiency increased cardiac HDL-C content compared with WT mice fed either with ND or with HFD. These results suggest that long-term HFD induced notable cardiac lipid deposition, which was remarkably reduced by *txnip* gene KO (Figs. 2C–G). Furthermore, cardiac function depends on the continuous supply of energy. Then, ATP content in the heart tissue was detected and the results showed that HFD caused a substantial decrease in ATP content of WT mice. However, TXNIP deficiency reversed the decreased ATP content in the heart of HFD mice with no alteration in mice with ND (Fig. 2H).

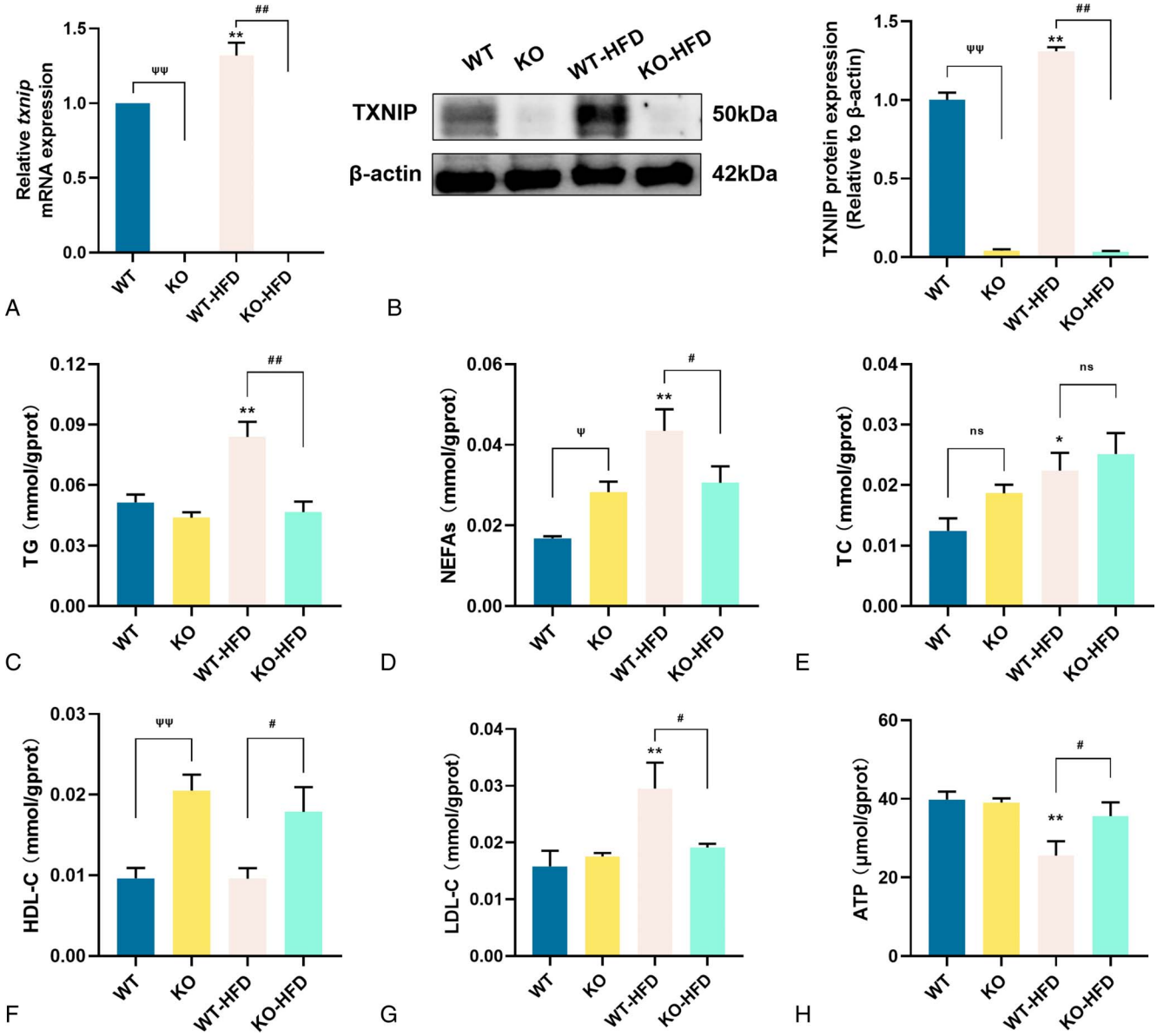

FIGURE 2. *Txnip* gene knockout ameliorated lipid deposition and energy supply disorder in heart. A, The mRNA level of *txnip* detected by RT-qPCR; mean ± SEM, n = 3. B, The protein level of TXNIP detected by Western blot; mean ± SEM, n = 6. C–G, Lipid concentrations in the heart tissue; mean ± SEM, n = 5. H, ATP content in the heart tissue; mean ± SEM, n = 3. $*P < 0.05$ & $**P < 0.01$ WT-HFD versus WT; $\psi P < 0.05$ and $\psi\psi P < 0.01$ KO versus WT; $\#P < 0.05$ and $\#\#P < 0.01$ KO-HFD versus WT-HFD; ns, not significant.

Txnip Gene KO Facilitated Cardiac FAO

Next, we explored the reason by which *txnip* gene KO ameliorated cardiac lipid deposition in mice. Cardiac lipid content is balanced by fatty acid supply and usage. Fatty acid translocase CD36 is essential for fatty acid uptake by binding to lipids and thus transporting lipids into cells.[32,33] Carnitine palmitoyl transferase 1 (CPT1) catalyzes the synthesis of acyl carnitine from acyl CoA (activated form of fatty acid) and carnitine to facilitate acyl carnitine enter to the mitochondrial matrix for oxidation. Carnitine palmitoyl transferase 1b (CPT1b) is the predominant CPT1 isoform in the heart.[34] Long-chain acyl-CoA dehydrogenase (ACADL), medium-chain acyl-CoA dehydrogenase (ACADM), and acyl-coenzyme A oxidase 1 (ACOX1) are rate-limiting enzymes for β-oxidation of fatty acids.[35] The results showed that the cardiac mRNA levels of *cd36*, *acadl*, and *acox1* in WT mice were significantly increased after 24 weeks of HFD. Besides, TXNIP deficiency increased the mRNA levels of *cd36*, *cpt1b*, *acadl*, *acadm*, and *acox1* compared with WT mice fed either with ND or with HFD (Figs. 3A–D). These findings suggest that *txnip* gene KO accelerated cardiac fatty acid uptake and oxidation, thereby contributing to the strain capacity of cardiomyocyte in a high-fat environment to balance lipid uptake and oxidation. Meanwhile, elevated fatty acid uptake and oxidation may result in oxidative stress.[18,36] Thus, SOD activity and MDA content, the two most commonly used index to evaluate oxidative stress, were assayed with commercial kits. Compared with the WT mice fed with ND, HFD inhibited cardiac SOD activity and increased MDA content in the heart tissue, although these alterations were significantly reversed by TXNIP deficiency (Figs. 3E, F). These results demonstrated that TXNIP deficiency promoted cardiac fatty acid uptake and oxidation while improved cardiac oxidative stress, especially in the context of long-term HFD.

Txnip Gene KO Elevated Cardiac Glucose Uptake and Glycolysis

In addition to fatty acids, glucose plays an integral role in the regulation of energy homeostasis in the heart. To this end, cardiac glucose metabolism was measured. Glucose transporter 1 and 4 (GLUT1/GLUT4) are the primary types of glucose transporter in heart tissues and participated in the glucose uptake only when they are translocated to the plasma membrane. The results showed that GLUT1 in the membrane fraction was significantly increased in the KO mice fed either with ND or with HFD compared with WT mice and reversed the reduction of GLUT1 in the membrane fraction caused by HFD (Fig. 4A). Meanwhile, the GLUT1 in the cytosol fraction showed quite opposite trends (Fig. 4B). These results indicated that *txnip* gene KO prevented the internalization of GLUT1 caused by the HFD (Figs. 4A, B). Differently, the protein expressions of GLUT4 in the membrane and cytosol fraction were both significantly reduced in WT-HFD group, whereas *txnip* gene KO reversed these trends (Figs. 4A, B). Hexokinase (HK), phosphofructokinase (PFK), and pyruvate kinase (PK) are key rate-limiting enzymes in glycolytic pathway.[37] The results showed that HFD decreased the cardiac mRNA levels of *pfkm* and *pkm* in WT mice, whereas TXNIP deficiency increased the mRNA levels of *hk2* and *pfkm* in mice fed with ND and increased the mRNA levels of *pfkm* and *pkm* in mice fed with HFD (Figs. 4C–E). These findings suggest that *txnip* gene KO could improve cardiac glucose uptake and glycolysis in mice that was impaired by a long-term HFD. Pyruvate dehydrogenase (PDH) is a key enzyme for aerobic glucose oxidation and loses its activity by phosphorylation at Ser 293 on the E1α subunit.[38] In our study, protein expression of PDH E1 component's α subunit (PDHE1α) and phosphorylation of PDHE1α (p-PDHE1α) at Ser-293 was measured. The results showed that *txnip* gene KO and HFD raised protein expression of p-PDHE1α/PDHE1α in WT mice, indicating reduced aerobic glucose oxidation in mice. However, TXNIP deficiency showed no alteration in p-PDHE1α/PDHE1α in the mice fed with HFD (see **Figure S3**, **Supplemental Digital Content**, http://links.lww.com/JCVP/A927).

Txnip Gene KO Improved Cardiac Mitochondrial Function in HFD Mice

To analyze the ultrastructure of cardiomyocytes, the heart tissue was observed via a transmission electron microscope. Our result showed an integrated spherical or oval shape and clear cristae of mitochondria in WT and KO mice fed with ND. However, we noticed that the heart of HFD WT mice showed an increase in mitochondrial volume density and damaged mitochondria with disarrayed cristae, and an increase in the lipid droplet density as well. These alterations caused by HFD feeding were all reversed by TXNIP deficiency (Figs. 5A–D). Given that change in mitochondrial membrane potential could reflect mitochondrial metabolic status,[39] JC-1 staining was performed. The results showed that *txnip* gene KO restored the mitochondrial membrane potential decreased by HFD feeding (Fig. 5E). In addition, the activity of mitochondrial respiratory chain complex Ⅴ (also known as ATP synthase) was detected to evaluate the oxidative phosphorylation efficiency of the cardiac mitochondria. The results showed that the complex Ⅴ activity was downregulated by HFD, whereas *txnip* gene KO improved the activity of complex Ⅴ (Fig. 5F). These results indicated that *txnip* gene KO could ameliorate mitochondrial injury caused by a long-term HFD.

Txnip Gene KO Regulated the Mitochondrial Dynamics in HFD Mice

Mitochondrial dynamics is associated with mitochondrial function and is regulated by mitochondrial fusion or fission proteins.[40] Mitofusin-1 protein (MFN1) and mitofusin-2 protein (MFN2) mediate the fusion of the outer mitochondrial membrane, and optic atrophy 1 (OPA1) mediates the fusion of the inner mitochondrial membrane.[41] Dynamin-related protein 1 (DRP1) can bind to mitochondrial outer membrane protein receptors such as mitochondrial fission 1 protein (FIS1) to promote mitochondrial fission.[42] These mitochondrial fusion or fission proteins were detected by Western blot assay. The results showed that cardiac DRP1 protein expression in the WT-HFD group was elevated than that in the WT group, whereas MFN2 protein expressions

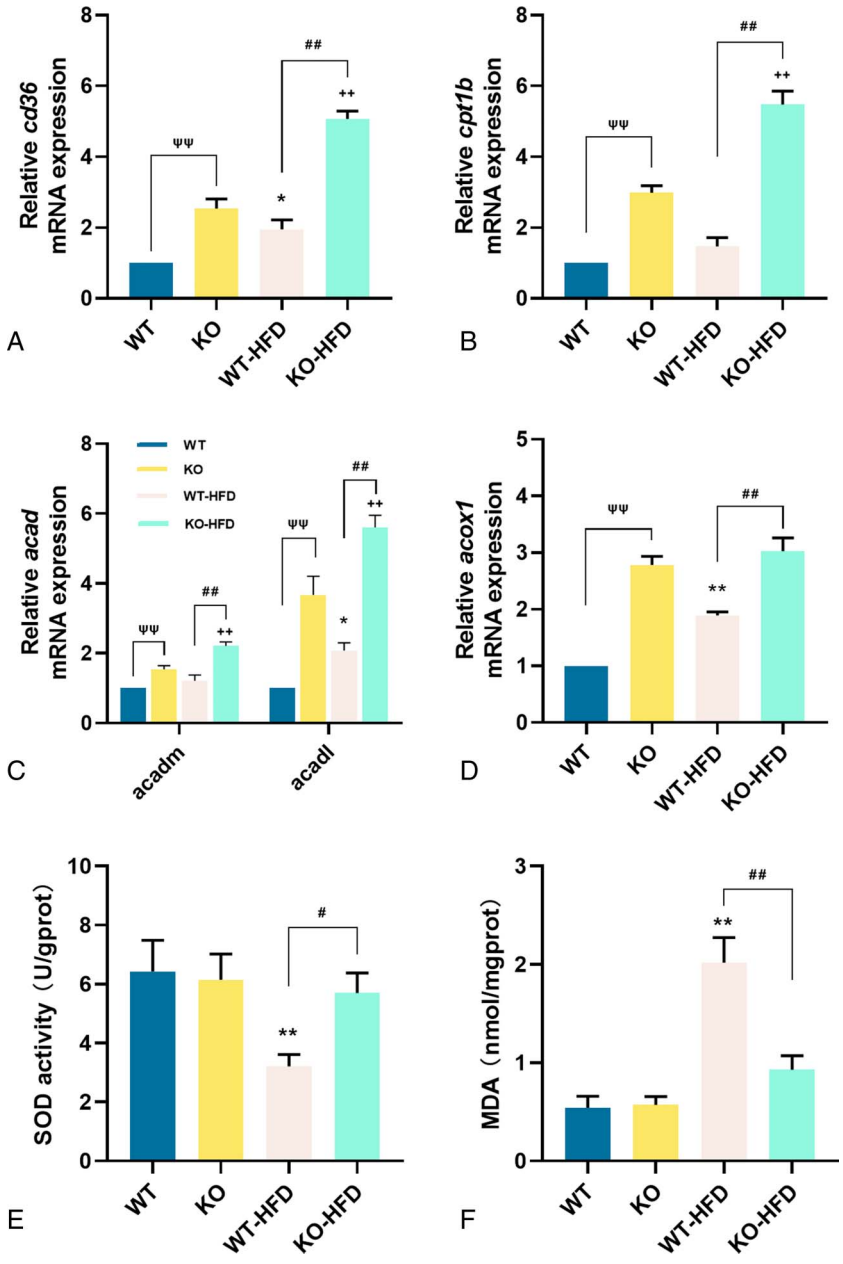

FIGURE 3. *Txnip* gene knockout improved the fatty acid oxidation capacity in heart. A–D, The mRNA levels of *cd36*, *cpt1b*, *acadm*, *acadl*, and *acox1* in the heart tissue detected by RT-qPCR; mean ± SEM, n = 4. E, SOD activity in the heart tissue; mean ± SEM, n = 5. F, MDA level in the heart tissue; mean ± SEM, n = 5. $*P < 0.05$ and $**P < 0.01$ WT-HFD versus WT; $\psi\psi P < 0.01$ KO versus WT; $\#P < 0.05$ and $\#\#P < 0.01$ KO-HFD versus WT-HFD; $++P < 0.01$ KO-HFD versus KO; ns, not significant.

were significantly decreased than those in the WT group. Although these alterations were significantly reversed by TXNIP deficiency. Meanwhile, MFN1, OPA1, and FIS1 protein expression was not statistically changed (Fig. 6). These results indicated that TXNIP deficiency could inhibit mitochondrial fission by decreasing DRP1 protein expression and promote mitochondrial fusion via upregulating MFN2 protein expression.

DISCUSSION

In recent years, the obesity epidemic accelerates the increase in the number of patients with obesity cardiomyopathy.[1] Here, we found that TXNIP was upregulated in the heart of mice with 24-week HFD feeding, whereas TXNIP deficiency prevented HFD-induced lipid accumulation and mitochondrial disorders in the heart, thereby ameliorating the cardiac function in obese mice. Mechanistically, TXNIP deficiency remodeled cardiac energy metabolism in HFD-fed mice by upregulating lipid uptake and FAO while promoting anaerobic glycolysis. Besides, TXNIP deficiency improved mitochondrial dysfunction via regulating mitochondrial fission and fusion in the context of chronic HFD feeding. Our work provides a theoretical basis for TXNIP exerting as a potential therapeutic target for the interventions of obesity cardiomyopathy.

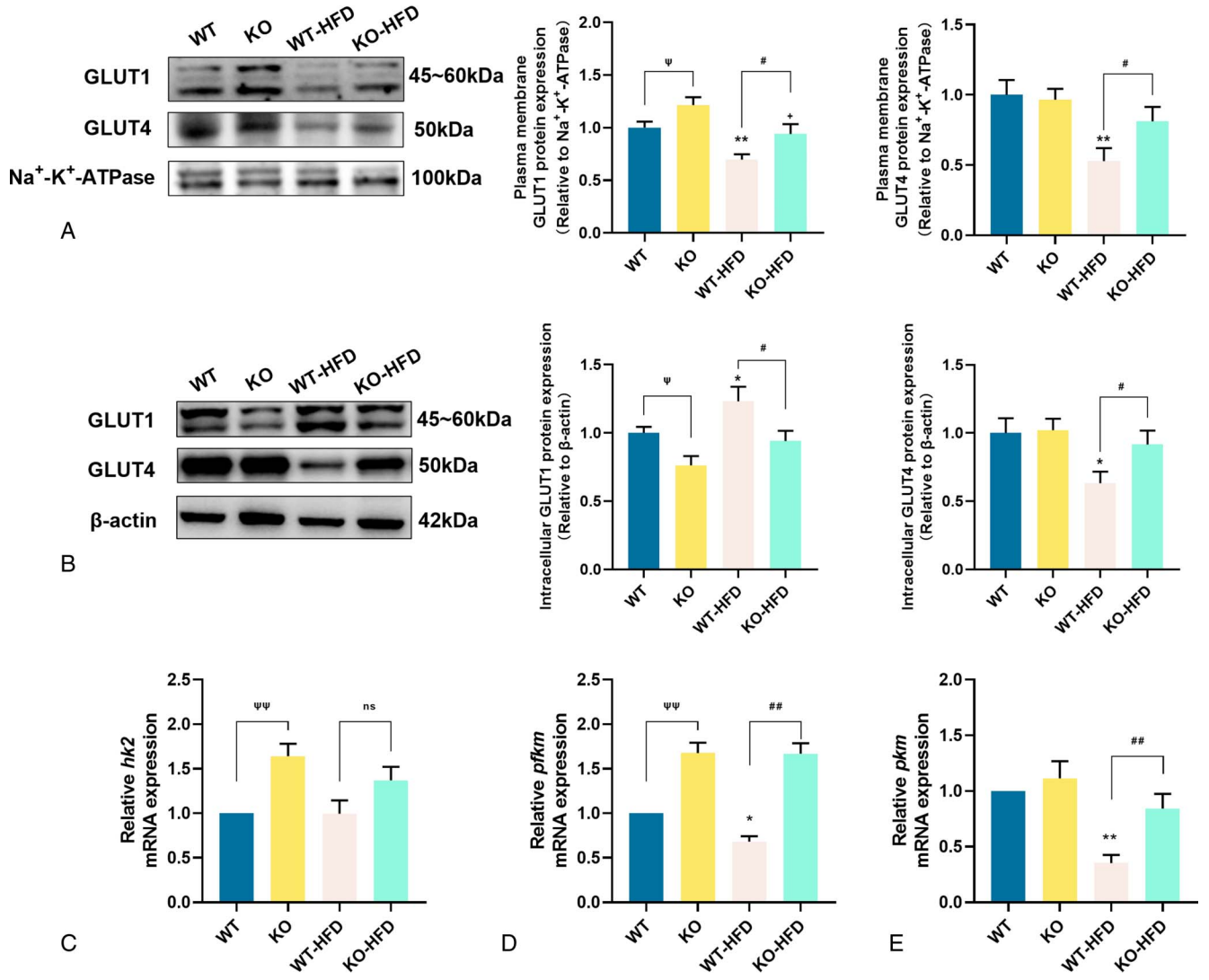

FIGURE 4. *Txnip* gene knockout improved the glucose uptake and glycolysis capacity in heart. A, The plasma membrane protein level of GLUT1 and GLUT4 detected by Western blot; mean ± SEM, n = 6. B, The intracellular protein level of GLUT1 and GLUT4 detected by Western blot; mean ± SEM, n = 6. C–E, The mRNA level of *hk2*, *pfkm*, and *pkm* detected by RT-qPCR; mean ± SEM, n = 4. *$P < 0.05$ and **$P < 0.01$ WT-HFD versus WT; ψ$P < 0.05$ and ψψ$P < 0.01$ KO versus WT; #$P < 0.05$ and ##$P < 0.01$ KO-HFD versus WT-HFD; +$P < 0.05$ KO-HFD versus KO; ns, not significant.

Chronic HFD leads to obesity cardiomyopathy and decline in cardiac function.[43] As shown in the present study, a decrease in LVEF and LVFS along with an increase in LVIDS and LVESV were found in the heart of 24-week HFD mice. However, TXNIP deficiency improved HFD-induced cardiac dysfunction, demonstrating its specific role in the intervention of obesity cardiomyopathy. It is well known that a long-term HFD will lead to large amount of lipid abnormally accumulates in the heart (also referred to as cardiac lipotoxicity), which is contributed to the progress of cardiac dysfunction.[7,9,18,44] Consistent with this, our results showed that chronic HFD increased the contents of TG, NEFAs, TC, and LDL-C in the heart. However, TXNIP deficiency improved the ectopic lipid deposition in the heart, indicating that TXNIP deficiency could protect cardiac function from lipotoxic damage.

Lipid in the heart is balanced by fatty acid uptake and oxidation. Our results showed that TXNIP deficiency further enhanced fatty acid uptake and FAO in the heart of HFD mice despite that HFD feeding elevated cardiac fatty acid uptake and FAO. Similarly, previous study demonstrated that cardiomyocyte-specific TXNIP KO could promote myocardial FAO via miR-33a signaling.[30] Excess cardiac FAO has long been considered to increase ROS production and subsequent oxidative stress damage.[19] Unexpectedly, our results showed that TXNIP deficiency ameliorated oxidative stress induced by HFD. These results demonstrated that TXNIP deficiency decreased lipid accumulation in the heart via upregulating cardiac fatty acid uptake and FAO and meanwhile improved oxidative stress under the condition of obesity. Indeed, TXNIP can bind to Trx, an intracellular antioxidant

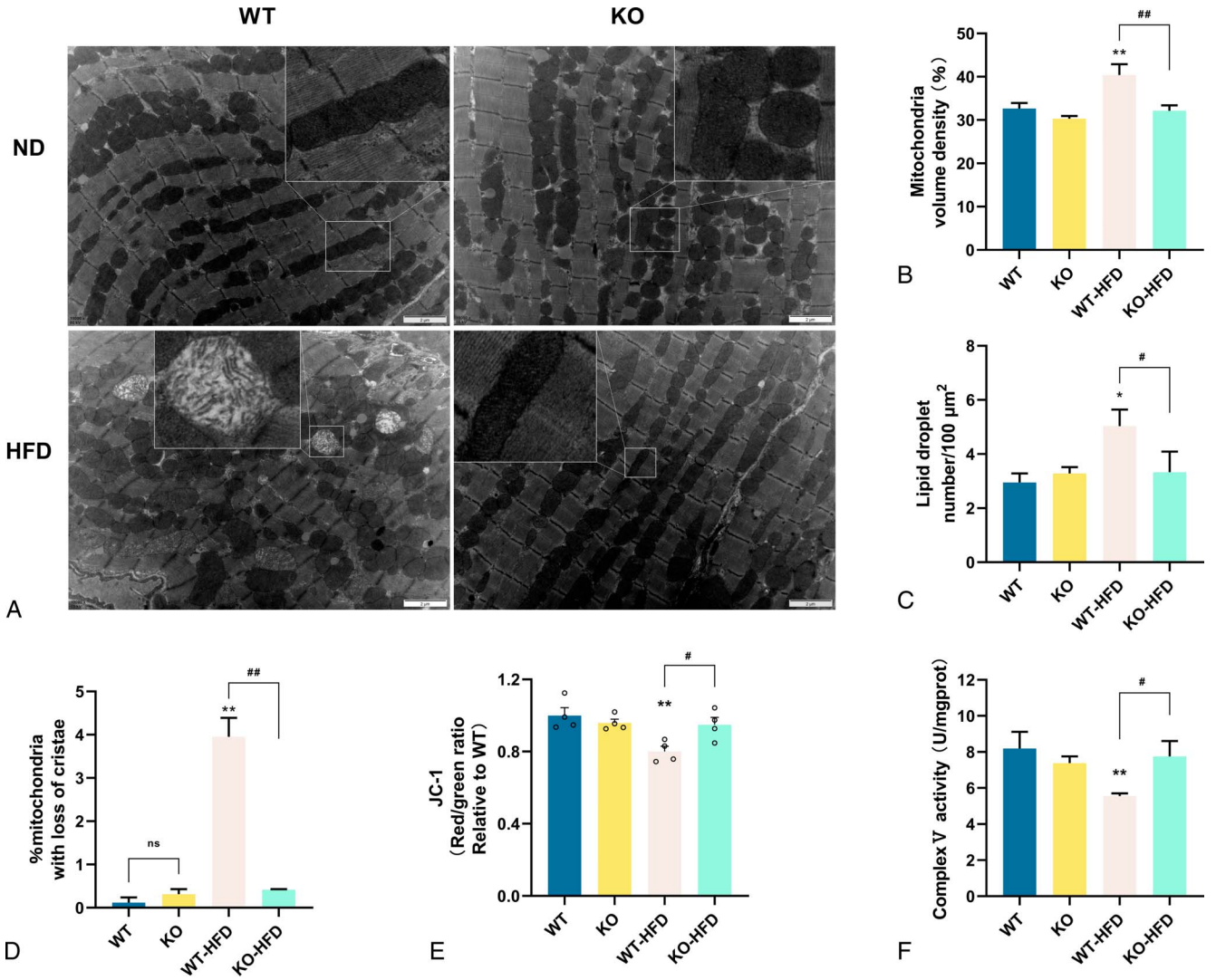

FIGURE 5. *Txnip* gene knockout ameliorated mitochondrial injury caused by a long-term HFD. A, Representative images of heart sections from electron microcopy. Scale bar, 2 μm. B, Mitochondrial density. Six random fields (×10,000) were analyzed per heart sample. C, Lipid droplet number. Six random fields (×10,000) were analyzed per heart sample. D, Percentage of mitochondria with loss of cristae. Six random fields (×10,000) were analyzed per heart sample. E, Mitochondrial membrane potential detected by JC-1 staining. F, Mitochondrial respiratory complex V activity; mean ± SEM, n = 3–4. $*P < 0.05$ and $**P < 0.01$ WT-HFD versus WT; $\#P < 0.05$ and $\#\#P < 0.01$ KO-HFD versus WT-HFD; ns, not significant.

system, and induce oxidative stress[45]; whereas TXNIP deficiency increased the antioxidant activity of Trx and thus improved oxidative stress. Besides, interventions that prevent the upregulation of FAO in obesity causes lipid accumulation and cardiac dysfunction,[9] and recent data showed that cardiac lipotoxicity is not attributable to increased FAO per se and increasing cardiac FAO could prevent HFD-induced cardiomyopathy,[9] illustrating that promoting cardiac FAO will be a promising strategy to protect the heart from lipotoxicity in obesity.

Increased FAO in mitochondria could competitively disrupt the oxidative capacity of glucose via fatty acid–glucose cycle.[46] In the present study, we found that HFD decreased the translocation of GLUT1 to the cell membrane and reduced the GLUT4 protein expression to restrict glucose uptake and increased PDH phosphorylation to inhibit glucose aerobic oxidation. However, it is notable that TXNIP deficiency promoted glucose uptake while inhibited glucose aerobic oxidation. Logically, inhibiting glucose oxidation will promoting glucose anaerobic glycolysis, a non–mitochondria-dependent energy supply mode for glucose. Our results showed that TXNIP deficiency significantly upregulated gene expressions of glycolysis-related enzyme, allowing the heart to change the metabolic flux of glucose to generate energy rapidly. TXNIP is considered as a switch of energy metabolism.[21] Inability of the mitochondria from high fat–fed rat hearts to use glucose resulted in the switch from glucose to FAO, indicating metabolic inflexibility in the heart of obesity.[47] Our results demonstrated that TXNIP deficiency promoted FAO and triggered the metabolic shift from glucose

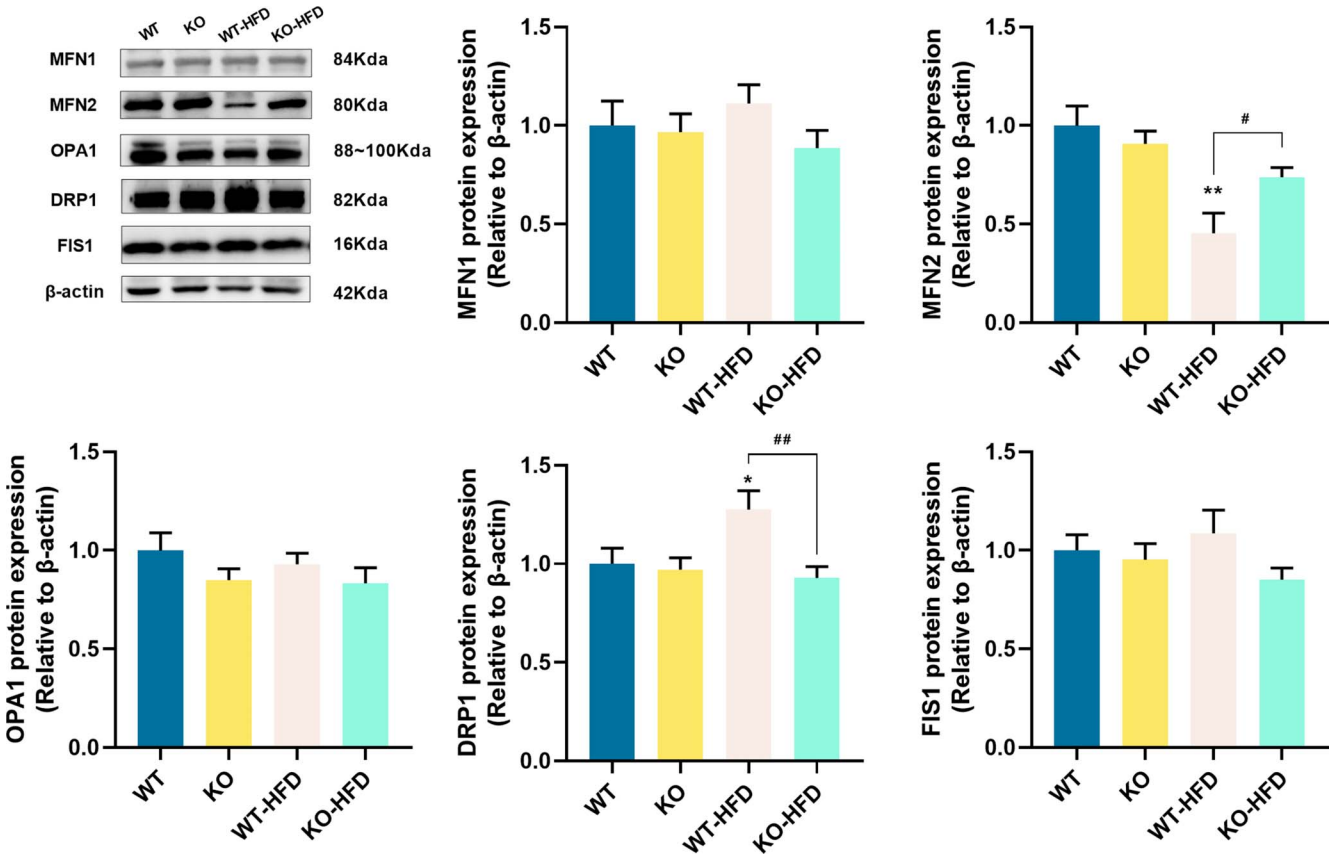

FIGURE 6. *Txnip* gene knockout regulated the expression of mitochondrial dynamics protein. The protein levels of MFN1, MFN2, OPA1, DRP1, and FIS1 in the heart tissue detected by Western blot; mean ± SEM, n = 6. $*P < 0.05$ and $**P < 0.01$ WT-HFD versus WT; $\#P < 0.05$ and $\#\#P < 0.01$ KO-HFD versus WT-HFD; ns, not significant.

oxidation to glycolysis, indicating the metabolic flexibility of energy source for heart.

Mitochondrial dysfunction is a culprit of obesity cardiomyopathy. The result of transmission electron microscopy on the heart showed that HFD caused mitochondrial damage. Consistent with this, 24-week HFD destroyed the mitochondrial membrane potential and decreased respiratory chain enzyme complex V activity. Mitochondria are the main site for lipid oxidation, and excess toxic lipid accumulation results in mitochondrial damage.[48,49] However, TXNIP deficiency promoted FAO and prevented lipid accumulation in the heart, which may contribute to ameliorate mitochondrial dysfunction, although enhanced FAO is considered to deteriorate mitochondrial function. This paradox led us to hypothesize that TXNIP deficiency increased cardiac FAO in obese mice may be owing to restored mitochondrial function. The mitochondrial dynamics is the core player involvement in mitochondrial function, and impairment in mitochondrial fission and/or fusion will lead to the obesity-related cardiomyocyte dysfunction.[50] Previous study has shown that a long-term HFD markedly decreased mitochondrial fusion proteins and increased mitochondrial fission proteins that caused mitochondrial dynamics disorder in the rat heart.[18] Similarly, our study showed a trend of decreased mitochondrial fusion and increased mitochondrial fission in mice fed with HFD. Mitochondrial fusion plays an important role in cardiac contractility, and a shift from fusion to fission induced by HFD feeding might contribute to the pathogenesis of cardiomyopathy.[51] Our results demonstrated that reversion of the shift from mitochondrial fusion to fission will offer cardioprotective effects in obesity.

Taken together, our results demonstrated that TXNIP deficiency improved mitochondrial dysfunction via elevating mitochondrial fusion and limiting excessive mitochondrial fission in the context of chronic HFD feeding, and thus promoting cardiac FAO to alleviate the ectopic lipid deposition in the heart of obese mice. Our findings provide evidence that TXNIP is a viable therapeutic target for the treatment of obesity cardiomyopathy.

REFERENCES

1. Blüher M. Obesity: global epidemiology and pathogenesis. *Nat Rev Endocrinol*. 2019;15:288–298.
2. Aghili SMM, Ebrahimpur M, Arjmand B, et al. Obesity in COVID-19 era, implications for mechanisms, comorbidities, and prognosis: a review and meta-analysis. *Int J Obes (Lond)*. 2021;45:998–1016.
3. Wong C, Marwick TH. Obesity cardiomyopathy: diagnosis and therapeutic implications. *Nat Clin Pract Cardiovasc Med*. 2007;4:480–490.
4. Kolwicz SC Jr, Purohit S, Tian R. Cardiac metabolism and its interactions with contraction, growth, and survival of cardiomyocytes. *Circ Res*. 2013;113:603–616.

5. Ren J, Wu NN, Wang S, et al. Obesity cardiomyopathy: evidence, mechanisms, and therapeutic implications. *Physiol Rev*. 2021;101:1745–1807.
6. Bertero E, Maack C. Metabolic remodelling in heart failure. *Nat Rev Cardiol*. 2018;15:457–470.
7. Belke DD, Larsen TS, Gibbs EM, Severson DL. Altered metabolism causes cardiac dysfunction in perfused hearts from diabetic (db/db) mice. *Am J Physiol-Endocrinol Metab*. 2000;279:E1104–E1113.
8. Mazumder PK, O'Neill BT, Roberts MW, et al. Impaired cardiac efficiency and increased fatty acid oxidation in insulin-resistant ob/ob mouse hearts. *Diabetes*. 2004;53:2366–2374.
9. Shao D, Kolwicz SC Jr, Wang P, et al. Increasing fatty acid oxidation prevents high-fat diet-induced cardiomyopathy through regulating Parkin-mediated Mitophagy. *Circulation*. 2020;142:983–997.
10. Yan J, Young ME, Cui L, et al. Increased glucose uptake and oxidation in mouse hearts prevent high fatty acid oxidation but cause cardiac dysfunction in diet-induced obesity. *Circulation*. 2009;119:2818–2828.
11. Goldberg IJ, Trent CM, Schulze PC. Lipid metabolism and toxicity in the heart. *Cell Metab*. 2012;15:805–812.
12. Peoples JN, Saraf A, Ghazal N, et al. Mitochondrial dysfunction and oxidative stress in heart disease. *Exp Mol Med*. 2019;51:1–13.
13. Ren J, Pulakat L, Whaley-Connell A, et al. Mitochondrial biogenesis in the metabolic syndrome and cardiovascular disease. *J Mol Med (Berl)*. 2010;88:993–1001.
14. Wold LE, Ceylan-Isik AF, Ren J. Oxidative stress and stress signaling: menace of diabetic cardiomyopathy. *Acta Pharmacologica Sinica*. 2005; 26:908–917.
15. Monserrat-Mesquida M, Quetglas-Llabrés M, Abbate M, et al. Oxidative stress and Pro-Inflammatory status in patients with non-Alcoholic fatty Liver disease. *Antioxidants (Basel)*. 2020;9:759.
16. Eisner V, Picard M, Hajnóczky G. Mitochondrial dynamics in adaptive and maladaptive cellular stress responses. *Nat Cell Biol*. 2018;20:755–765.
17. Wu NN, Zhang Y, Ren J. Mitophagy, mitochondrial dynamics, and homeostasis in cardiovascular aging*Oxid Med Cell Longev*. 2019;2019: 9825061.
18. Chen D, Li X, Zhang L, et al. A high-fat diet impairs mitochondrial biogenesis, mitochondrial dynamics, and the respiratory chain complex in rat myocardial tissues. *J Cell Biochem*. 2018;119:9602.
19. Tsushima K, Bugger H, Wende AR, et al. Mitochondrial reactive oxygen species in lipotoxic hearts induce post-translational Modifications of AKAP121, DRP1, and OPA1 that promote mitochondrial fission. *Circ Res*. 2018;122:58–73.
20. Yamawaki H, Haendeler J, Berk BC. Thioredoxin: a key regulator of cardiovascular homeostasis. *Circ Res*. 2003;93:1029–1033.
21. Yoshihara E. TXNIP/TBP-2: a Master regulator for glucose homeostasis. *Antioxidants (Basel)*. 2020;9:765.
22. Sullivan WJ, Mullen PJ, Schmid EW, et al. Extracellular matrix remodeling regulates glucose metabolism through TXNIP destabilization. *Cell*. 2018;175:117–132.e21.
23. Wu N, Zheng B, Shaywitz A, et al. AMPK-dependent degradation of TXNIP upon energy stress leads to enhanced glucose uptake via GLUT1. *Mol Cell*. 2013;49:1167–1175.
24. Oka Si, Yoshihara E, Bizen-Abe A, et al. Thioredoxin binding protein-2/ thioredoxin-interacting protein is a critical regulator of insulin secretion and peroxisome proliferator-activated receptor function. *Endocrinology*. 2009;150:1225–1234.
25. Yoshioka J, Chutkow WA, Lee S, et al. Deletion of thioredoxin-interacting protein in mice impairs mitochondrial function but protects the myocardium from ischemia-reperfusion injury. *J Clin Invest*. 2012; 122:267–279.
26. Yoshioka J, Lee RT. Thioredoxin-interacting protein and myocardial mitochondrial function in ischemia-reperfusion injury. *Trends Cardiovasc Med*. 2014;24:75–80.
27. Xiang G, Seki T, Schuster MD, et al. Catalytic degradation of vitamin D up-regulated protein 1 mRNA enhances cardiomyocyte survival and prevents left ventricular remodeling after myocardial ischemia. *J Biol Chem*. 2005;280:39394–39402.
28. Yoshioka J, Imahashi K, Gabel SA, et al. Targeted deletion of thioredoxin-interacting protein regulates cardiac dysfunction in response to pressure overload. *Circ Res*. 2007;101:1328–1338.
29. Yoshioka J, Schulze PC, Cupesi M, et al. Thioredoxin-interacting protein controls cardiac hypertrophy through regulation of thioredoxin activity. *Circulation*. 2004;109:2581–2586.
30. Chen J, Young ME, Chatham JC, et al. TXNIP regulates myocardial fatty acid oxidation via miR-33a signaling. *Am J Physiol-Heart Circ Physiol*. 2016;311():H64–H75.
31. Szczepaniak LS, Victor RG, Orci L, Unger RH. Forgotten but not gone: the rediscovery of fatty heart, the most common unrecognized disease in America. *Circ Res*. 2007;101:759–767.
32. Douglas Braymer H, Zachary H, Schreiber AL, et al. Lingual CD36 and nutritional status differentially regulate fat preference in obesity-prone and obesity-resistant rats. *Physiol Behav*. 2017;174:120–127.
33. Feng L, Gu C, Li Y, Huang J. High glucose promotes CD36 expression by upregulating peroxisome proliferator-activated receptor γ levels to exacerbate lipid deposition in renal tubular cells. *Biomed Res Int*. 2017;2017:1414070.
34. He L, Kim T, Long Q, et al. Carnitine palmitoyltransferase-1b deficiency aggravates pressure overload-induced cardiac hypertrophy caused by lipotoxicity. *Circulation*. 2012;126:1705–1716.
35. Zhang F, Xiong Q, Tao H, et al. ACOX1, regulated by C/EBPα and miR-25-3p, promotes bovine preadipocyte adipogenesis. *J Mol Endocrinol*. 2021;66:195–205.
36. Aronis A, Madar Z, Tirosh O. Mechanism underlying oxidative stress-mediated lipotoxicity: exposure of J774.2 macrophages to triacylglycerols facilitates mitochondrial reactive oxygen species production and cellular necrosis. *Free Radic Biol Med*. 2005;38:1221–1230.
37. Basse AL, Isidor MS, Winther S, et al. Regulation of glycolysis in brown adipocytes by HIF-1α. *Sci Rep*. 2017;7:4052.
38. Fan J, Kang HB, Shan C, et al. Tyr-301 phosphorylation inhibits pyruvate dehydrogenase by blocking substrate binding and promotes the Warburg effect. *J Biol Chem*. 2014;289:26533–26541.
39. Zhang L, Dong L, Yang L, et al. MiR-27a-5p regulates acrylamide-induced mitochondrial dysfunction and intrinsic apoptosis via targeting Btf3 in rats. *Food Chem*. 2022;368:130816.
40. Scott I, Youle RJ. Mitochondrial fission and fusion. *Essays Biochem*. 2010;47:85–98.
41. Yue W, Chen Z, Liu H, et al. A small natural molecule promotes mitochondrial fusion through inhibition of the deubiquitinase USP30. *Cell Res*. 2014;24:482–496.
42. Yeon JY, Min SH, Park HJ, et al. Mdivi-1, mitochondrial fission inhibitor, impairs developmental competence and mitochondrial function of embryos and cells in pigs. *J Reprod Dev*. 2015;61:81–89.
43. Tong M, Saito T, Zhai P, et al. Alternative Mitophagy protects the heart against obesity-associated cardiomyopathy. *Circ Res*. 2021;129:1105–1121.
44. Wende AR, Abel ED. Lipotoxicity in the heart. *Biochim Biophys Acta*. 2010;1801:311–319.
45. Yoshihara E, Masaki S, Matsuo Y, et al. Thioredoxin/Txnip: redoxisome, as a redox switch for the pathogenesis of diseases. *Front Immunol*. 2014; 4:514.
46. Hue L, Taegtmeyer H. The Randle cycle revisited: a new head for an old hat. *Am J Physiol Endocrinol Metab*. 2009;297:E578–E591.
47. Cole MA, Murray AJ, Cochlin LE, et al. A high fat diet increases mitochondrial fatty acid oxidation and uncoupling to decrease efficiency in rat heart. *Basic Res Cardiol*. 2011;106:447–457.
48. Mazibuko-Mbeje SE, Dludla PV, Johnson R, et al. Aspalathin, a natural product with the potential to reverse hepatic insulin resistance by improving energy metabolism and mitochondrial respiration. *PLoS One*. 2019; 14:e0216172.
49. Abdul-Ghani MA, Muller FL, Liu Y, et al. Deleterious action of FA metabolites on ATP synthesis: possible link between lipotoxicity, mitochondrial dysfunction, and insulin resistance. *Am J Physiology-Endocrinology Metab*. 2008;295():E678–E685.
50. Forte M, Schirone L, Ameri P, et al. The role of mitochondrial dynamics in cardiovascular diseases. *Br J Pharmacol*. 2021;178: 2060–2076.
51. Eisner V, Cupo RR, Gao E, et al. Mitochondrial fusion dynamics is robust in the heart and depends on calcium oscillations and contractile activity. *Proc Natl Acad Sci USA*. 2017;114:E859–E868.